International Journal of Transport Development and Integration
https://www.acadlore.com/journals/IJTDI

Energy Demand and Solar Charging Feasibility of Off-Grid Hybrid Electric Motorcycles for Rural Applications

Christian Soolany[1*], Dhimas Oki Permata Aji[1], Sigit Suwarto[1], Setya Permana Sutisna[2], Furqon[2], Purwoko Hari Kuncoro[2]

[1] Mechanical Engineering Department, Nahdlatul Ulama Al Ghazali University, 53274 Cilacap, Indonesia
[2] Agricultural Engineering Department, Jenderal Soedirman University, 53122 Purwokerto, Indonesia

[*] Correspondence: Christian Soolany (christian.fti@unugha.ac.id)

Received: 09-11-2025 **Revised:** 03-09-2026 **Accepted:** 03-19-2026

Citation: C. Soolany, D. O. P. Aji, S. Suwarto, S. P. Sutisna, Furqon, and P. H. Kuncoro, "Energy demand and solar charging feasibility of off-grid hybrid electric motorcycles for rural applications," *Int. J. Transp. Dev. Integr.*, vol. 10, no. 2, pp. 342–352, 2026. https://doi.org/10.56578/ijtdi100202.

Abstract: Rural electric mobility in Indonesia remains constrained by limited charging infrastructure and unreliable access to grid electricity, particularly in remote areas where motorcycles are the dominant mode of daily transport. At the same time, Indonesia has strong year-round solar energy potential due to its equatorial location. Although solar photovoltaic (PV) charging has been widely recognised as a promising option for off-grid mobility, limited research has examined its suitability for hybrid electric motorcycles (HEM) under actual rural operating conditions. This study combines field measurements and simulation-based modelling to evaluate the daily energy demand of HEM and to assess the feasibility of PV-assisted off-grid charging in rural Central Java, Indonesia. The analysis shows that daily energy demand ranges from 1.2–1.5 kWh, depending on terrain, payload, and travel speed. Simulation results indicate that a system consisting of a 200 Wp PV module, a 1.5 kWh battery, and regenerative braking support can satisfy approximately 87% of daily energy demand during the rainy season and 97% during the dry season. These findings demonstrate the technical potential of solar-assisted HEM for rural transport and provide practical reference values for the design of decentralised off-grid charging systems.

Keywords: Hybrid electric motorcycle; Solar energy; Off-grid; Rural mobility; Energy demand; System simulation

1 Introduction

The global shift toward sustainable transportation becomes inevitable due to the need to curb greenhouse gas emissions, reduce fossil fuel dependency, and mitigate climate change impacts. Electric vehicles (EVs) have received widespread attention as a clean mobility solution, supported by rapid advancements in battery technology, power electronics, and renewable energy integration [1]. However, EV deployment remains uneven, which is largely more concentrated in well-developed urban regions where charging infrastructure and stable electricity supply are available [2] rather than in rural areas.

In Indonesia, particularly in remote areas, motorcycles are the dominant mode of transportation due to their affordability, maneuverability, and suitability for the unpaved or narrow rural roads [3]. However, reliance on this motorcycle with an internal combustion engine (ICE) system results in more fuel consumption, emissions, and user dependence on unstable and costly fuel distribution systems [4, 5].

On the other hand, fully electric motorcycles appear as a more environmentally friendly alternative. However, the fully electric motorcycles' reliance on grid-based charging presents limitations in off-grid regions characterized by unreliable electricity access, long charging cycles, and unavailability of technical support [6]. For these reasons, hybrid electric motorcycles (HEM) may promote a more realistic transitional technology by offering electric propulsion efficiency due to the operational resilience maintenance under infrastructure limitations [7, 8].

For the equatorial region like Indonesia with a sufficient solar irradiation throughout the year, solar photovoltaic (PV) charging technology presents a promising renewable option for off-grid mobility [9]. Despite of this, previous studies remain two major existing research gaps: (i) theoretical gap—previous studies primarily discuss solar-powered or electric two-wheelers applications without taking into account the real rural operational variables such as terrain

variation, payload, and speed dynamics [10]; and (ii) practical gap—there is limitation on empirical data and sizing guidelines for PV–battery configurations specifically for rural motorcycle application [11].

Therefore, this study proposes an integrated empirical–simulation approach that combines field-based energy demand measurements across multiple terrain types and hybrid PV–battery–regenerative braking system modeling. The study is expected to provide a data-driven energy demand model and optimal off-grid PV sizing recommendation specifically for rural HEMs applications. Thus, the study is further expected to enable context-appropriate design development rather than simply performing extrapolation from urban EV assumptions. The outcomes are expected to serve as a replicable framework for decentralized community-based rural e-mobility planning development.

2 Methodology

This study adopted a three-stage sequential framework consisting of (i) rural mobility and environmental data acquisition, (ii) empirical energy-consumption testing, and (iii) modelling and simulation of the standalone PV–battery–regenerative configuration.

2.1 Study Area and Research Design

The research was conducted in rural areas of Cilacap and Banyumas Regencies, Central Java, Indonesia, where motorcycles represent the primary mode of transportation for daily commuting, agricultural logistics, and goods delivery. These areas were selected due to limited charging infrastructure, mixed road surfaces, and variable terrain profiles, which are representative of off-grid motorcycle usage conditions [12]. A field-based empirical-simulation hybrid research design was employed to capture both real-world energy-demand characteristics and techno-economic feasibility of off-grid solar-assisted charging scenarios.

2.2 Phase 1: Rural Mobility and Solar Resource Data Acquisition

A structured survey was conducted among active daily motorcycle users using purposive sampling. Collected variables included trip frequency, travel distance, dominant terrain type, payload mass, travel time windows, and fuel cost. The derived mean daily travel distance served as the baseline energy-demand factor for subsequent analysis.

To characterize site-specific renewable energy availability, a pyranometer was deployed to record global horizontal irradiance (GHI) at one-minute intervals across representative dry- and rainy-season periods. Ambient temperature and relative humidity were recorded simultaneously due to their influence on PV cell efficiency. The GHI data were post-processed to obtain daily average solar energy ($\mathrm{kWh \cdot m^{-2} \cdot day^{-1}}$), seasonal variation bands, and hourly irradiance profiles, which were used as boundary conditions for the PV-output model.

2.3 Phase 2: Experimental Energy-Consumption Measurement

Empirical energy-consumption measurements were performed using a 110-cc motorcycle operated under controlled field trials across three terrain categories: asphalt, unpaved, and hilly routes, with two payload conditions (single rider and rider plus 30–60 kg load). An inline DC power analyser (Egteks Mpower 1203; accuracy $\pm 0.5\%$ reading ± 2 digits, $\pm 0.2\%$ voltage, $\pm 0.8\%$ current) was installed between the battery and controller to measure real-time electrical parameters (voltage, current, and instantaneous power). Data were logged at 10 Hz to capture transient load events, including acceleration, deceleration, slope transitions, and surface condition changes.

Prior to deployment, the analyser was calibrated using a certified DC power source with $\pm 0.2\%$ accuracy and cross-checked using an IEC-61010-compliant multimeter. Each terrain-speed-load scenario was repeated three times, and results were reported as mean values following outlier removal using an interquartile range (IQR) threshold of $\pm 10\%$ from the median.

2.4 Phase 3: Hybrid Energy-System Modelling Framework

A standalone solar-assisted hybrid charging system integrating a PV module, lithium-ion battery, and regenerative braking subsystem was modelled using empirical inputs obtained from Phases 1 and 2. The PV subsystem was modelled based on measured GHI profiles, module efficiency, and derating factors including temperature impact, dust deposition, cable losses, and partial shading. The battery subsystem was modelled using rated capacity, depth-of-discharge (DoD), round-trip efficiency, and dynamic SOC limits, while the regenerative subsystem was modelled using kinetic-energy recovery functions based on braking and downhill operation probability [13].

2.5 Mathematical Modelling and Governing Equations

The modelling approach employed vehicle longitudinal-dynamics and energy-balance principles to derive mechanical-to-electrical energy demand, PV-generation potential, regenerative-energy recovery, and SOC evolution. The key governing equations are presented in Eqs. (1)–(10), along with corresponding variable definitions and SI units. The feasibility criterion was defined as:

To account for real-world uncertainties, a seasonal stochastic assessment was performed by simulating dry-season and rainy-season irradiance profiles based on local pyranometer measurements and validated meteorological data. Variability in energy demand was also considered through distance-range fluctuation derived from the rural mobility survey. System reliability was evaluated based on the percentage of daily energy demand met under both seasonal conditions while maintaining SOC above the specified threshold.

The mathematical formulation presented in this section aims to establish a deterministic relationship between the motorcycle's mechanical energy demand, the electrical energy supplied by the PV–battery–regenerative system, and the State-of-Charge (SOC) evolution throughout daily operation. All governing equations were derived based on fundamental vehicle longitudinal dynamics and energy balance principles. The modelling approach integrates terrain-induced resistance, real-world driving conditions, and component conversion efficiencies to accurately represent off-grid operational scenarios.

The total mechanical energy demand required for propulsion was computed by summing four primary resistive forces: aerodynamic drag, rolling resistance, road gradient force, and inertial acceleration [14]. These forces collectively reflect the characteristics of rural driving conditions, where variations in surface type, slope, and speed are more prevalent than in urban settings. The corresponding vehicle force model is expressed as Eq. (1).

$$E_{road} = \int (F_{aero} + F_{rolling} + F_{grade} + F_{acc}) \cdot v(t) \mathrm{d}t \tag{1}$$

where, F_{aero} accounts for air resistance, $F_{rolling}$ represents losses due to surface friction, F_{grade} captures the effect of uphill or downhill motion, and F_{acc} models' transient acceleration demands.

Mechanical energy demand was converted into electrical energy demand through the drivetrain efficiency to reflect the energy drawn from the battery (Eq.(2)).

$$E_{el} = \frac{E_{road}}{\eta_{driveterain}} \tag{2}$$

To estimate the renewable energy harvested, the instantaneous PV output power was simulated using irradiance data as a time-varying boundary condition, defined as Eq. (3).

$$P_{PV}(t) = G(t) \cdot A_{cell} \cdot \eta_{cell} \cdot \eta_{sys} \tag{3}$$

where, η_{sys} incorporates inverter, wiring, and temperature losses. The daily PV energy yield was obtained via numerical integration over a 24-hour window (Eq. (4)).

$$E_{PV,day} = \int_{1}^{24} P_{PV}(t) \mathrm{d}t \tag{4}$$

Regenerative braking energy recovery was integrated into the model to represent kinetic energy recovery during deceleration and downhill motion (Eq. (5)).

$$P_{regen}(t) = \eta_{regen} \cdot mgh(t) \tag{5}$$

The dynamic SOC tracking model was implemented using a forward-time update rule (Eq. (6)).

$$\mathrm{SOC}(t+1) = \mathrm{SOC}(t) + \frac{P_{in}(t) - P_{out}(t)}{E_{bat,rated}} \tag{6}$$

where, the minimum SOC is 20%.

Finally, system feasibility for each scenario was evaluated using the following daily energy sufficiency criterion (Eq. (7)).

$$E_{PV,day} + E_{regen,day} + E_{battery} \geq E_{demand} \tag{7}$$

To identify the optimal configuration, a computational model integrating PV, battery, and regenerative braking subsystems was developed. The model was designed to simulate energy flows between system components under various rural operating scenarios, using empirical input data collected from field measurements.

The PV subsystem was modelled using measured irradiance profiles, module efficiency, and derating factors including temperature effect, dust deposition, and partial shading. The lithium-ion battery model incorporated rated capacity, DoD, round-trip efficiency, and SOC boundary constraints (20–80%). The regenerative braking subsystem was formulated using kinetic energy recovery [15], defined in Eq. (10), to estimate recoverable deceleration and downhill energy.

The minimum required battery capacity (C_{bat}) was estimated using Eq. (8).

$$E_{PV,day} + E_{regen,day} + E_{battery} \geq E_{demand} \tag{8}$$

where, V_{nom} is the nominal battery voltage and D_{od} is the permissible depth of discharge.

The required PV area for standalone energy sufficiency was computed using Eq. (9) [16].

$$A_{PV} = \frac{E_m}{G_{av}\eta_{PV}t_{sun}} \tag{9}$$

where, G_{av} representing the average solar irradiance (W/m^2), η_{PV} the panel efficiency, and t_{sun} the effective daily sunshine hours.

Recoverable regenerative braking energy was estimated using Eq. (10).

$$E_{rb} = \frac{1}{2}mv^2\eta_{rb} \tag{10}$$

where m is the mass of the motorcycle and rider, v is the average deceleration velocity, and $\eta_{r\beta}$ is the recovery efficiency of the regenerative system.

2.6 Simulation Protocol and Assumptions

Simulation was conducted using Scilab 6.1.1 with a time-step of one minute, matching the irradiance logging interval. Seasonal simulations were executed using dry- and rainy-season irradiance profiles. Battery initial SOC was set to 80%, and the minimum allowable SOC was 20% to prevent deep-cycle degradation. Sensitivity analysis was performed on panel capacity, battery capacity, and regenerative-efficiency parameters. Table 1 lists the physical, electrical, and environmental parameters used in modelling, along with data sources, manufacturer specifications, and empirical measurement basis. Only parameters with traceable sources were used, and no estimated or assumed values were included without justification.

Table 1. Parameter values and data sources used for modelling

Parameter	Value/Range	Unit	Source/Basis	Notes
Gravity	9.81	m/s^2	Physical constant	-
Air density	1.184	kg/m^3	American Society of Heating, Refrigerating and Air-Conditioning Engineers (ASHRAE) standard (27 °C, 1 atm)	Local tropical condition
Drag coefficient	0.9	-	Motorcycle aero literature	Small scooter profile
Rolling resistance	0.0150.030	-	Empirical range (paved vs unpaved)	Road-dependent
Frontal area	0.6	m^2	Estimated + manufacturer profile	Rider included
Motordrivetrain efficiency	0.80–0.90	-	Typical brushless direct current (BLDC) + chain transmission	-
Regenerative efficiency	0.20–0.60	-	Literature [15] assumed sensitivity	Simulation parameter
Panel efficiency	0.18	-	Module datasheet	Monocrystalline
Sunshine duration	4–6	hours/day	Local pyranometer data	Seasonal variability
Battery depth-of-discharge (DoD)	0.8	-	Manufacturer	To preserve life cycle
State-of-Charge (SOC) initial	0.8	-	Simulation assumption	Standard battery management system (BMS) practice
Sampling rate	10	Hz	Logger spec	Real-time logging

Model outputs were validated by comparing simulated electrical energy-consumption values (Wh·km^{-1}) with experimentally measured values from Phase 2 using the mean absolute percentage error (MAPE). A validation

acceptance threshold of MAPE $< 10\%$ was adopted, indicating acceptable model fidelity for feasibility and sizing evaluation.

3 Results and Discussion

3.1 Rural Motorcycle Usage Characteristics

The household mobility survey identified that rural motorcycle users performed an average of three daily trips with a mean total travel distance of 15 km/day and a typical riding duration of 1.0–1.5 hours/day (Table 2). The primary mobility purposes included commuting to workplaces or schools (34%), household errands (28%), and agricultural or trading-related transportation (38%). In addition, 45–62% of respondents reported carrying additional payloads ranging from 30–60 kg, mostly consisting of agricultural products, tools, or packaged goods.

Table 2. Summary of rural motorcycle usage patterns obtained from household mobility survey (N = 100)

Variable	Category Distribution (%)	Mean/Median Value*	Notes/Interpretation
Daily trip frequency	1–2 trips (22%), 34 trips (68%), >4 trips (10%)	3 trips/day (mode)	Frequent short–loop mobility
Daily travel distance	<10 km (18%), 1020 km(64%),>20 km (18%)	15 km/day (median)	Short–medium distance usage
Daily riding duration	<1 h (24%), 1–2 h (58%), >2 h (18%)	1.5 h/day	Combined commuting & logistics
Transported load type	None (20%), Passenger (42%), Goods (38%)	-	Goods: agricultural & household
Additional load mass	0–30 kg (46%), 30–60 kg (42%), >60 kg (12%)	35 kg (approx. mean)	Influences drivetrain duty cycle
Road condition exposure	Asphalt (55%), Unpaved (30%), Hilly (15%)	Mixed	Terrain variability dominant
Average operational speed	<20 km/h (18%), 20–40 km/h (72%), >40 km/h (10%)	25–35 km/h	Terrain & payload–dependent
Preferred charging period	Night (72%), Day (10%), Irregular (18%)	-	Driven by grid availability
Derived energy requirement	-	1.2–1.5 kWh/day	Based on usage + conversion factors

Note: *household mobility survey

Unlike urban users who generally travel on paved roads with predictable routes and minimal payload, rural users operate across mixed terrain, non-linear routing, and load-bearing conditions, which collectively influence drivetrain duty cycles and energy demand patterns. Previous urban studies in Indonesia and Asia report average motorcycle travel distances between 18–25 km/day with limited or no-load carriage [17, 18] indicating that rural usage patterns are operationally more demanding despite having similar or shorter travel distances. These characteristics demonstrate that distance alone is not a sufficient predictor of energy demand in rural settings; instead, terrain heterogeneity and load carriage must be incorporated into propulsion energy modelling and system sizing. Consequently, the 15 km/day value derived from this survey was selected as the empirical baseline for subsequent energy testing and simulation.

In addition to multifunctional use, mobility behaviour was strongly influenced by road surface conditions, with users reporting route exposure consisting of 55% asphalt, 30% unpaved soil, and 15% hilly terrain. Mixed-terrain exposure is known to increase rolling resistance, energy dissipation, and throttle modulation variability [19], which is reflected in the empirical operational riding speed range of 25–35 km/h. These values represent a safety- and terrain-imposed compromise rather than performance-driven selection, aligning with rural off-grid mobility characteristics reported in other developing regions [20].

Collectively, these findings confirm that rural motorcycle operation is multi-functional, terrain-dependent, and load-variable, forming a distinct usage profile that differs significantly from urban two-wheeler operation typically referenced in EV design literature. Therefore, distance-only estimations are insufficient for modelling rural energy demand, and terrain heterogeneity, payload frequency, and operational speed modulation must be incorporated into propulsion and hybrid system sizing. Based on the median value and distribution stability, 15 km/day was selected as the representative empirical baseline for subsequent experimental measurement and simulation scenarios.

3.2 Energy Consumption Across Operating Conditions

Empirical measurements demonstrated substantial variability in energy demand across combined terrain, speed, and load scenarios, ranging from 28 Wh·km^{-1} on low-speed asphalt to 92 Wh·km^{-1} on hilly terrain with payload (Table 3), representing an approximately 230% increase between the lowest and highest consumption conditions. Relative to asphalt conditions, unpaved and hilly routes exhibited 1.4–1.9 times higher energy consumption, while payload addition elevated energy demand by 12–18% under comparable speeds. The reported standard deviation (SD) values further indicate that hilly and loaded scenarios exhibited greater dispersion, implying increased variability and reduced predictability of energy consumption.

These results are consistent with longitudinal dynamics principles, where increased rolling resistance, gravitational load components, and throttle modulation under uneven terrain contribute to higher mechanical-to-electrical energy conversion requirements [12]. Comparable findings were documented in off-road EV assessments, though such studies predominantly focus on all-terrain or recreational EVs rather than daily commuter motorcycles [19, 21], highlighting a contextual research gap addressed by this study.

Further analysis of the measured data suggests a positive and near-linear correlation between payload magnitude and propulsion energy demand within the tested range. Across all terrains and within the operational speed category of 20–40 km/h, the addition of 30–60 kg increased energy consumption by an average of 12–18%, which corresponds to an estimated incremental gradient of approximately 0.55–0.85 Wh·km^{-1} per 10 kg of additional load. This proportional trend is aligned with light electric vehicle traction models that indicate a direct relationship between gross mass and rolling resistance contribution [22]. Although the present analysis is limited to two discrete payload ranges, the derived gradient provides a practical estimation parameter for rural HEM energy-modelling and PV battery sizing in load-dependent scenarios.

Collectively, these results confirm that terrain type and payload characteristics function as primary determinants of energy consumption rather than secondary modifiers, particularly in rural mobility environments. Therefore, rural EV or HEM energy-demand prediction models must incorporate terrain–speed–load coupling, rather than adopting uniform or distance-only estimation approaches commonly used in urban mobility studies.

Table 3. Energy consumption of motorcycles under diverse operating conditions

Terrain Type	Speed Level	Load Condition	Average Energy Consumption (Wh/km)*	Standard Deviation (SD, Wh/km)*	N*
Asphalt	Low (<20 km/h)	Single rider	28	1.80	3
	Medium (20–40 km/h)	Single rider	41	0.29	3
	High (>40 km/h)	Single rider	55	2.40	3
	Medium (20–40 km/h)	Rider + 30–60 kg load	48	2.82	3
	High (=40 km/h)	Rider + 30–60 kg load	65	2.72	3
Unpaved	Low (<20 km/h)	Single rider	39	0.95	3
	Medium (20–40 km/h)	Single rider	52	0.71	3
	High (>40 km/h)	Single rider	70	1.94	3
	Medium (20–40 km/h)	Rider + 30–60 kg load	62	1.90	3
	High (>40 km/h)	Rider + 30–60 kg load	82	6.80	3
Hilly	Low (<20 km/h)	Single rider	50	2.53	3
	Medium (20–40 km/h)	Single rider	68	3.82	3
	High (>40 km/h)	Single rider	85	3.34	3
	Medium (20–40 km/h)	Rider + 30–60 kg load	78	4.78	3
	High (>40 km/h)	Rider + 30–60 kg load	92	2.96	3

Note: *derived from experimental measurements

3.3 Solar Irradiance Potential and Seasonal Variability

Field-based solar resource assessment indicated high average daily irradiance values ranging from 4.2–5.1 kWh·m^{-2}·day^{-1}, producing a corresponding specific PV yield of 3.9–4.8 kWh·kWp^{-1}·day^{-1} for the study location (Table 4). Although irradiance slightly decreased during the rainy season, the values remained above the practical minimum threshold for small-scale PV charging applications. These findings suggest that rural open-field environments offer better solar exposure than typical urban installations, which commonly yield 3.5–4.0 kWh·kWp^{-1} day^{-1} due to shading, aerosols, and infrastructure obstructions. The results align with national resource maps and empirical studies confirming that tropical low-latitude regions maintain stable year-round solar availability [21].

Table 4. Average daily solar irradiance and photovoltaic (PV) output

Parameter	Value	Notes
Solar irradiance (kWh/m^2/day)	4.2–5.1	Field measurement, rural site
PV installed capacity (Wp)	200	Monocrystalline module
Average PV output (Wb/day)	780–950	Seasonal variation
Specific yield (kWh/kWW/day)	3.9–4.8	Higher than urban benchmarks

Seasonal analysis further indicated that the dry season (June–September) produced the highest resource availability with irradiance levels exceeding 5.0 kWh·m^{-2}·day^{-1}, while the wet season (December–March) showed moderately reduced values of 4.2–4.5 kWh·m^{-2}·day^{-1} due to cloud cover and elevated humidity (Table 5). However, even under wet seasonal conditions, irradiance remained adequate to support off-grid PV applications.

Table 5. Characteristics of solar energy resources in Cilacap and Banyumas Regencies, Indonesia

Condition/Period	Average Daily Irradiance (kWh/m^2/day)*	Peak Irradiance (W/m^2)*	Minimum Irradiance (W/m^2)*	Remarks
Dry season (Jun–Sep)	5.2 $\pm$ 0.115	>900 (around noon)	<150 (early morning/late afternoon)	Clear sky, high solar potential
Wet season (Dec–Mar)	4.3 $\pm$ 0.087	~800 (around noon)	<100 (during cloudy/rainy periods)	Frequent clouds, moderate potential
Annual average	4.8 $\pm$ 0.115	850–900	100–150	Stable year–round potential, minor seasonal variability
Daily profile	Bell-shaped distribution	Peak: 10:00–14:00	Low: 06:00–08:00, 16:00–18:00	Consistent with tropical climate

Note: *experimental measurements

Figure 1 shows representative diurnal irradiance and PV output curves for a 200 Wp monocrystalline module. Both seasons exhibit a bell-shaped profile with peak irradiance occurring around 10:00–14:00, reaching 850–900 W·m^{-2} during dry-season clear-sky conditions and 700–800 W·m^{-2} during the wet season. Corresponding maximum PV output reached 160–180 W (dry season) and 130–150 W (wet season) after applying derating factors. Integrated daily production ranged between 900–950 Wh/day and 780–820 Wh/day, respectively, validating the specific yield estimates presented in Table 5.

Overall, the local solar resource demonstrates high seasonal reliability and provides sufficient generation potential to support daily off-grid charging autonomy for HEM, provided that an appropriately sized storage buffer is incorporated in system design. Thus, PV sizing should prioritize wet-season worst-case irradiance profiles rather than mean annual metrics, as this approach minimizes the probability of operational failure for rural daily-use mobility [23].

3.4 Hybrid System Performance Evaluation

The simulation results confirmed that PV capacity and battery storage size had the most dominant influence on daily energy sufficiency, while regenerative braking served as an auxiliary contributor to enhance net available energy (Table 6). The 200 Wp–1.5 kWh–40% regenerative braking configuration achieved >97% daily energy autonomy under dry-season conditions and >87% under rainy-season conditions, while maintaining SOC above the 20% operational safety threshold throughout the diurnal cycle. This configuration, therefore, represents the minimum reliable system size capable of supporting daily off-grid mobility operation.

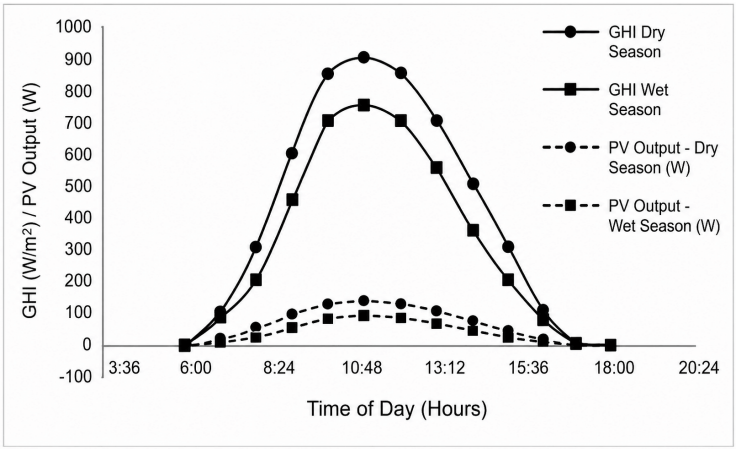

Figure 1. Daily solar irradiance (GHI) and simulated photovoltaic (PV) output profiles for a 200 Wp monocrystalline module under representative dry-season and rainy-season conditions in Cilacap, Indonesia

Table 6. Summary of hybrid energy system simulation results

Photovoltaic Capacity (W)	Battery Capacity (kWh)	Regen. Braking Efficiency (%)	Demand Met-Dry Season (%)	Demand Met-Rainy Season (%)	Equivalent Fuel Consumption (L/day)
150	1	0	87–92	60–67	0.28
150	1	40	92–94	68–72	0.25
200	1	40	95–98	82–88	0.22
200	1.5	40	97–100	87–92	0.22
250	1	40	98–100	90–95	0.21

Increasing the PV and battery size beyond 250 Wp/2.0 kWh demonstrated diminishing performance improvements of $<$8%, despite adding cost, mass, and installation footprint. Conversely, configurations below 150 Wp/1.0 kWh consistently failed to maintain SOC above the safe limit, particularly during rainy-season scenarios, indicating heightened sensitivity to seasonal irradiance variability. In these undersized systems, regenerative braking improved energy sufficiency, but remained insufficient to compensate for the baseline energy deficit, reiterating its role as a supplementary rather than primary charging source [20].

3.5 Energy Balance Analysis

The daily energy balance assessment (Table 7) shows that the PV subsystem generated 832 Wh/day during dry-season conditions and 638 Wh/day during rainy-season conditions, supplemented by 180 Wh/day and 140 Wh/day of regenerative energy, respectively. The remaining demand was supplied by the battery without resulting in unmet load events, and the minimum SOC consistently remained above the 20% safety limit throughout the cycle (Figure 2).

Table 7. Daily energy balance values

Parameter/Season	Dry Season (Wh/day)	Rainy Season (Wh/day)
Daily Energy Demand	1300	1300
Photovoltaic (PV) Energy Supply	832	638
Regenerative Braking Energy	180	140
Battery Energy Contribution	288	522
Energy Deficit/Surplus	0 (balanced)	0 (balanced)

Table 7 summarizes the energy flow associated with the recommended 200 Wp–1.5 kWh–40% regen hybrid configuration. Under dry-season conditions, PV generation supplied approximately 64% of the total daily energy requirement, followed by regenerative braking (14%) and battery discharge (22%). In contrast, during the rainy season, PV contribution declined to approximately 49%, increasing the reliance on the battery (40%) due to reduced solar input, even though regenerative braking maintained a similar proportional contribution (11%). Despite this

seasonal shift, the hybrid configuration achieved zero daily energy deficit, confirming that the selected system capacity provides sufficient buffering margin to accommodate weather-induced energy variability [22].

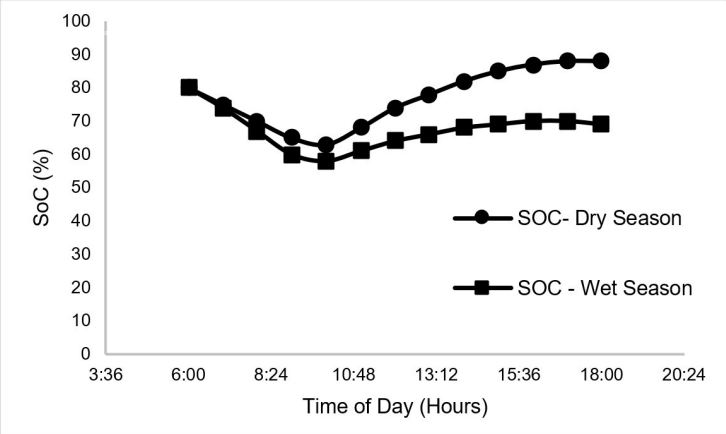

Figure 2. Simulated daily State-of-Charge (SOC) profiles of the 1.5 kWh battery for the 200 Wp PV–battery–regenerative system configuration under representative dry-season and rainy-season operating conditions in rural Cilacap

Figure 2 illustrates the SOC trajectories for both seasonal profiles. During the dry season, SOC reduction remained shallow and exhibited rapid midday recovery due to higher PV availability, whereas during the rainy season, SOC recovery was slower and discharge deeper, but remained within safe operational limits. These SOC behaviors corroborate the energy sufficiency results and underline the role of regenerative braking as a stabilizing auxiliary rather than a primary source of daily recharge.

In addition to confirming energy sufficiency, the results highlight an important insight regarding seasonal operational resilience. While dry-season operation is clearly self-sustaining with minimal dependence on stored energy, rainy-season performance demonstrates that the system continues to operate within safe energy margins, albeit with a higher proportion of battery utilization. This indicates that battery sizing rather than PV oversizing becomes the dominant factor for maintaining operational continuity during low-irradiance periods, particularly in regions experiencing extended rainy-season durations.

Furthermore, the SOC profiles indicate that the system avoids deep discharge cycles, which is beneficial for maintaining battery longevity and minimizing capacity fade [24]. Maintaining SOC above 20% throughout the operational window aligns with common lithium battery management recommendations and is expected to reduce degradation rates associated with DoD stress and thermal cycling. These findings imply that operational stress on the battery remains within acceptable technical boundaries, supporting long-term deployment feasibility.

The comparative contribution of regenerative braking, which supplied 11–14% of total daily energy, also indicates that mechanical energy recovery plays a meaningful stabilizing role, particularly during the early morning and post-commute recovery period when irradiance is still rising [25]. Although it is insufficient as a primary charging mechanism, its consistent contribution across seasons provides an inherent buffer against short-term intermittence, improving operational smoothness and charge sustainability without requiring additional infrastructure.

Finally, when interpreted from an implementation perspective, these energy balance outcomes suggest that rural deployment should prioritize conservative sizing based on wet-season conditions rather than annual averages, and incorporate battery-focused reliability planning, such as thermal management, exposure protection, and periodic state-of-health (SOH) monitoring. Such strategies are expected to enhance field robustness and lifecycle performance, particularly in environments where technical maintenance resources are limited.

4 Conclusions

This study empirically validated the technical feasibility of integrating PV systems with HEMs to support off-grid rural mobility. Field-based surveys and controlled measurements indicated that rural users require 1.2–1.5 kWh/day, with energy consumption strongly influenced by terrain type, payload, and operating speed, rather than travel distance alone. Solar resource assessment showed consistently high irradiance levels of 4.2–5.1 kWh·m^{-2}·day^{-1}, confirming the suitability of PV-based charging infrastructure in rural tropical environments.

Simulation results demonstrated that a 200 Wp PV–1.5 kWh battery–40% regenerative braking configuration is capable of fulfilling >97% of daily energy demand during dry-season conditions and >87% during rainy-season conditions while maintaining safe SoC limits. This configuration achieved the best performance-to-cost-to-weight

trade-off, whereas larger systems achieved marginal performance gains at the expense of increased capital cost, mass, and installation complexity.

Overall, the findings establish that solar-assisted HEMs represent a technically viable and context-appropriate solution for rural transportation electrification, offering improved energy autonomy and reduced dependence on fossil fuels. The results also provide empirical design parameters that can be used as a reference for future rural EV planning and decentralized charging development.

Future research should focus on: (i) multi-objective techno-economic optimization incorporating lifetime cost and degradation factors, (ii) experimental validation of long-term battery cycling under PV-dominated profiles, and (iii) evaluation of shared or community-based PV charging models to enhance scalability and socio-economic adoption potential.

Author Contributions

Conceptualization, C.S. and S.P.S.; methodology, C.S. and D.O.P.A.; software, C.S.; validation, C.S., D.O.P.A., and S.S.; formal analysis, C.S. and D.O.P.A.; investigation, C.S., D.O.P.A., and S.S.; resources, S.P.S., F., and P.H.K.; data curation, C.S. and D.O.P.A.; writing—original draft preparation, C.S.; writing—review and editing, C.S., S.S., S.P.S., and F.; visualization, C.S. and D.O.P.A.; supervision, S.P.S. and P.H.K.; project administration, C.S.; funding acquisition, C.S. and S.P.S. All authors have read and agreed to the published version of the manuscript.

Funding

The Ministry of Higher Education, Science, and Technology (KEMENDIKTISAINTEK), through the Directorate of Research and Community Service (DPPM), based on Decree Number 0419/C3/DT.005.00/2025 and Agreements/Contracts Number 127/C3/DT.05.00/PL/2025; 037/LL6/PL/AL.04/2025; 070/Ybk.041.14/PT/2025, for funding under the Regular Fundamental Research Scheme.

Data Availability

The data used to support the research findings are available from the corresponding author upon request.

Conflicts of Interest

The authors declare no conflict of interest.

References

[1] C. A. Kusuma, M. Multifiah, and W. Syafitri, "The influence of urbanization and socio-economic conditions to vehicle ownership in developing city," *J. Bina Praja*, vol. 10, no. 2, pp. 287–302, 2018. https://doi.org/10.21787/jbp.10.2018.287-302

[2] C. Soolany, "Rekayasa energi terbatukan pompa air bertenaga surya menggunakan switch remote control wireless," *J. Agricultural and Biosystem Eng. Res.*, vol. 3, no. 2, pp. 67–76, 2023. https://doi.org/10.20884/1.jaber.2022.3.2.8410

[3] T. Eccarius and C. C. Lu, "Powered two-wheelers for sustainable mobility: A review of consumer adoption of electric motorcycles," *Int. J. Sustain. Transp.*, vol. 14, no. 3, pp. 215–231, 2020. https://doi.org/10.1080/15568318.2018.1540735

[4] C. Soolany, S. Suwarto, D. O. P. Aji, F. A. Azzizzah, and D. Pamungkas, "Implementasi konversi sepeda motor bensin manual menjadi sepeda motor listrik yang ramah lingkungan," *J. Ilm. Momentum*, vol. 20, no. 1, pp. 42–48, 2024. https://doi.org/10.36499/jim.v20i1.10823

[5] Ministry of Energy and Mineral Resources, Republic of Indonesia, "Handbook of energy and economic statistics of Indonesia 2022," Renewable Energy and Energy Conservation (ESDM), 2023. https://www.esdm.go.id/assets/media/content/content-handbook-of-energy-and-economic-statistics-of-indonesia-2022.pdf

[6] G. Rituraj, G. R. C. Mouli, and P. Bauer, "A comprehensive review on off-grid and hybrid charging systems for electric vehicles," *IEEE Open J. Ind. Electron.*, vol. 3, pp. 203–222, 2022. https://doi.org/10.1109/OJIES.2022.3167948

[7] J. De Cauwer, W. Verbeke, T. Coosemans, S. Faid, and J. Van Mierlo, "A data-driven method for energy consumption prediction and energy-efficient routing of electric vehicles in real-world conditions," *Energies*, vol. 10, no. 5, p. 608, 2017. https://doi.org/10.3390/en10050608

[8] F. Mwasilu, J. J. Justo, E. K. Kim, T. D. Do, and J. W. Jung, "Electric vehicles and smart grid interaction: A review on vehicle to grid and renewable energy sources integration," *Renew. Sustain. Energy Rev.*, vol. 34, pp. 501–516, 2014. https://doi.org/10.1016/j.rser.2014.03.031

[9] A. Bugaje, M. Ehrenwirth, C. Trinkl, and W. Zoerner, "Investigating the performance of a rural off-grid photovoltaic system with electric-mobility solutions: A case study based on Kenya," *J. Sustain. Dev. Energy Water Environ. Syst.*, vol. 10, no. 1, pp. 1–15, 2022. https://doi.org/10.13044/j.sdewes.d9.0391

[10] M. M. Rahman, M. A. H. Baky, A. K. M. S. Islam, and M. A. Al-Matin, "A techno-economic assessment for charging easy bikes using solar energy in Bangladesh," in *2016 4th International Conference on the Development in the in Renewable Energy Technology (ICDRET)*, Dhaka, Bangladesh, 2016, pp. 1–5. https://doi.org/10.1109/ICDRET.2016.7421487

[11] M. R. Elkadeem, S. Wang, S. W. Sharshir, and E. G. Atia, "Feasibility analysis and techno-economical design of grid-isolated hybrid renewable energy system for electrification of agriculture in developing countries: A case study in Dongola, Sudan," *Energy Convers. Manag.*, vol. 196, pp. 1453–1478, 2019. https://doi.org/10.1016/j.enconman.2019.06.085

[12] Y. A. Rokhim, C. Soolany, D. O. P. Aji, S. Suwarto, and V. Listanto, "Studi perakitan sepeda listrik: Identifikasi komponen utama dan proses untuk kinerja optimal," *AME (Apl. Mek. Energi) J. Ilm. Tek. Mesin*, vol. 11, no. 1, pp. 49–53, 2025. https://doi.org/10.32832/ame.v11i1.1402

[13] M. Rezkallah, A. Hamadi, A. Chandra, and B. Singh, "Design and implementation of active power control with improved P&O method for wind-PV-battery-based standalone generation system," *IEEE Trans. Ind. Electron.*, vol. 65, no. 7, pp. 5590–5600, 2018. https://doi.org/10.1109/TIE.2017.2777404

[14] S. Pance, D. Piskac, A. Bures, A. Voldrich, M. Kovac, and B. A. Budiman, "Evaluation of motorcycle energy consumption in urban traffic," *Int. J. Sustain. Transp. Technol.*, vol. 2, no. 1, pp. 27–31, 2019. https://doi.org/10.31427/ijstt.2019.2.1.4

[15] M. M. Cheepinapi, J. Morla, N. K. Pichuka, A. Shaik, J. P. Veeramuchu, K. B. Padaga, and S. S. M. Hashmi, "Design and fabrication of regenerative braking system," *Int. J. Multidiscip. Res.*, vol. 5, no. 3, pp. 1–7, 2023. https://doi.org/10.36948/ijfmr.2023.v05i03.2775

[16] B. Dilla, B. Widi, S. Wilyanti, A. Jaenul, Z. M. Antono, and A. Pangestu, "Implementasi solar charge controller untuk pengisian baterai dengan menggunakan sumber energi hybrid pada sepeda motor listrik," *J. Edukasi Elektro*, vol. 6, no. 2, pp. 128–135, 2022. https://doi.org/10.21831/jee.v6i2.53327

[17] A. F. Aritenang, "The crucial role of motorcycle-based ride-hailing among commuters: The case of Jakarta and Bandung in metropolitan areas," *J. Public Transp.*, vol. 26, p. 100082, 2024. https://doi.org/10.1016/j.jpubtr.2024.100082

[18] H. Iseki and M. Tingstrom, "A new approach for bikeshed analysis with consideration of topography, street connectivity, and energy consumption," *Comput. Environ. Urban Syst.*, vol. 48, pp. 166–177, 2014. https://doi.org/10.1016/j.compenvurbsys.2014.07.008

[19] T. B. Joewono, B. Z. Lauw, and H. Hendy, "Motorcycle in the West Java Province, Indonesia: Its growth and characteristics," *Civ. Eng. Dimens.*, vol. 15, no. 1, pp. 61–70, 2013. https://doi.org/10.9744/ced.15.1.61-70

[20] U. Datta, A. Kalam, and J. Shi, "Battery energy storage system control for mitigating PV penetration impact on primary frequency control and state-of-charge recovery," *IEEE Trans. Sustain. Energy*, vol. 11, no. 2, pp. 746–757, 2020. https://doi.org/10.1109/TSTE.2019.2904722

[21] D. F. Silalahi, A. Blakers, M. Stocks, B. Lu, C. Cheng, and L. Hayes, "Indonesia's vast solar energy potential," *Energies*, vol. 14, no. 17, p. 5424, 2021. https://doi.org/10.3390/en14175424

[22] Z. Yi and P. H. Bauer, "Effects of environmental factors on electric vehicle energy consumption: A sensitivity analysis," *IET Electr. Syst. Transp.*, vol. 7, no. 1, pp. 3–13, 2017. https://doi.org/10.1049/iet-est.2016.0011

[23] H. Fathabadi, "Novel solar/wind-powered electric vehicle charging station with vehicle-to-grid (V2G) capability," *Energy Convers. Manag.*, vol. 105, pp. 439–450, 2015. https://doi.org/10.1016/j.enconman.2016.12.045

[24] N. R. Chowdhury, A. J. Smith, K. Frenander, A. Mikheenkova, R. W. Lindström, and T. Thiringer, "Influence of state of charge window on the degradation of Tesla lithium-ion battery cells," *J. Energy Storage*, vol. 76, p. 110001, 2024. https://doi.org/10.1016/j.est.2023.110001

[25] M. Mahmoud, M. Ramadan, A. G. Olabi, K. Pullen, and S. Naher, "A review of mechanical energy storage systems combined with wind and solar applications," *Energy Convers. Manag.*, vol. 210, p. 112670, 2020. https://doi.org/10.1016/j.enconman.2020.112670